Charmonia production in p+p collisions under NRQCD formalism

Vineet Kumar[1,2] and Prashant Shukla[1,2,*]

[1]*Nuclear Physics Division, Bhabha Atomic Research Center, Mumbai, India*

[2]*Homi Bhabha National Institute, Anushakti Nagar, Mumbai, India*

(Dated: March 22, 2016)

Abstract

In this work we calculate the high p_T quarkonia production cross section using NRQCD formalism. In NRQCD formalism quarkonia cross-section can be written as a product of short distance QCD cross-sections and long distance matrix elements (LDMEs). The short distance cross-sections can be calculated in terms of perturbative QCD and LDMEs are obtained using experimental data. We use measured data of $\psi(2S)$, χ_c and J/ψ in p+p and p + $\bar{p}$ collisions at 1.8, 1.96, 7 and 8 TeV to constrain LDMEs. These LDMEs are then used to calculate charmonia cross-section in p+p collisions at 13 and 14 TeV.

_____

[*] pshukla@barc.gov.in

I. INTRODUCTION

The quarkonia ($Q\bar{Q}$) have provided useful tools for probing both perturbative and non-perturbative aspects of Quantum Chromodynamics (QCD) eversince the discovery of J/ψ resonance [1, 2]. Quarkonia states are qualitatively different from most other hadrons since the velicity v of the heavy constituents is small which allows a non-relativistic treatment. The quarkonia production process can be divided into two major parts

1. Production of a heavy quark pair in hard partonic collisions.

2. Formation of quarkonia from the two heavy quarks.

The heavy quarks due to their high mass ($m_c \sim 1.6$ GeV/c^2, $m_b \sim 4.5$ GeV/c^2), are produced in initial partonic collisions with sufficiently high momentum transfers. Thus the heavy quark production can be treated perturbatively [3, 4]. The formation of quarkonia out of the two heavy quarks is nonperturbative process and is treated in terms of different models [5, 6]. Most notable models for quarkonia production are the color-singlet model (CSM), the color-evaporation model (CEM), the non-relativistic QCD (NRQCD) factorization approach, and the fragmentation-function approach.

In the CSM [7–10], it is assumed that the $Q\bar{Q}$ pair that evolves into the quarkonium is in a color-singlet state and has the same spin and angular-momentum quantum numbers as the quarkonium. The production rate of quarkonium state is related to the absolute values of the color-singlet $Q\bar{Q}$ wave function and its derivatives, evaluated at zero $Q\bar{Q}$ separation. These quantities can be extracted by comparing theoretical expressions for quarkonium decay rates in the CSM with experimental measurements. The CSM was successful in predicting quarkonium production rates at relatively low energy [11] but, at high energies, very large corrections to the CSM appear at next-to-leading order (NLO) and next-to-next-to-leading order (NNLO) in α_s [12–14]. As we will describe below, the NRQCD factorization approach encompasses the color-singlet model, but goes beyond it. In the CEM [15–17], it is assumed that the produced $Q\bar{Q}$ pair evolves into a quarkonium if its invariant mass is less than the threshold for producing a pair of open-flavor heavy mesons. The nonperturbative probability for the $Q\bar{Q}$ pair to evolve into a quarkonium state is fixed by comparison with the measured total cross section for the production of that quarkonium state. The CEM predictions provide good descriptions of the CDF data for J/ψ, $\psi(2S)$, and χ_c production

at $\sqrt{s} = 1.8$ TeV [17] but it fails to predict the quarkonium polarization.

In the NRQCD factorization approach [5] the probability for a $Q\bar{Q}$ pair to evolve into a quarkonium is expressed as matrix elements of NRQCD operators in terms of the heavy-quark velocity v in the limit $v \ll 1$. This approach takes into account the complete structure of the $Q\bar{Q}$ Fock space, which is spanned by the state $n = {}^{2S+1}L_J^{[a]}$ with definite spin S, orbital angular momentum L, total angular momentum J, and color multiplicity a $= 1$ (colour-singlet), 8 (color-octet). The $Q\bar{Q}$ pairs which are produced at short distances in color-octet (CO) states, subsequently evolve into physical, color-singlet (CS) quarkonia by the nonperturbative emission of soft gluons. In the limit $v \to 0$, the traditional CS model (CSM) is recovered in the case of S-wave quarkonia.

The NRQCD gives good description of the measured J/ψ yield [23–25] although the J/ψ polarization, unravel a rather confusing pattern [21–23], It has been shown that the set of CO LDMEs fitted to p_T distributions measured at HERA and CDF lead to very good descriptions of the p_T distributions from RHIC and the LHC [24]. On the other hand, the Tevatron data alone is not sufficient to constrain all the CO LDMEs [25] also the fit results of Ref. [24] and Ref [25] are incompatible with each other.

In last few years, there has been some progress on the NLO QCD calculations. The NLO corrections to color-singlet J/ψ hadroproduction have been investigated in Refs. [13, 18]. The J/ψ production is found to be enhanced by 2-3 order of magnitude at high p_T region, and its polarization changes from transverse into longitudinal at NLO [18]. The NLO corrections to J/ψ production via S-wave color octet (CO) states (${}^1S_0^{[8]}\,{}^3S_1^{[8]}$) are studied in Ref. [19] and the corrections to p_T distributions of both J/ψ yield and polarization are found to be small. In Refs. [20], NLO corrections for χ_{cJ} hadroproduction are also studied. The NLO calculations are still evolving and thus we use LO calculations in this work.

With the LHC running for several years we now have very high quality quarkonia production data in several kinamatic regions up to very high transeverse momentum. In this paper, we use new data from LHC [26–28] along with the available data from CDF [30, 31] to constrain the LDMEs. These new LDMEs are then used to predict the J/ψ and $\psi(2S)$ cross-section at 13 TeV for the kinematical bins relevant to LHC detectors.

3

II. QUARKONIA PRODUCTION IN P+P COLLISIONS

The NRQCD formalism provides a theoretical framework for studying the heavy quarkonium production. The dominant processes in the production of heavy mesons ψ are $g + q \to \psi + q$, $q + \bar{q} \to \psi + g$ and $g + g \to \psi + g$. We label theese processes as $a + b \to \psi + X$, where a and b are the light incident partons. The invariant cross-section for the production of ψ can be written in factorized form as

$$E\frac{d^3\sigma^\psi}{d^3p} = \sum_{a,b} \int \int dx_a \, dx_b \, G_{a/p}(x_a, \mu_F^2) \, G_{b/p}(x_b, \mu_F^2) \frac{\hat{s}}{\pi} \frac{d\sigma}{d\hat{t}} \otimes \delta(\hat{s} + \hat{t} + \hat{u} - M^2), \quad (1)$$

where $G_{a/p}(G_{b/p})$ is the distribution function (PDF) of the incoming parton $a(b)$ in the incident proton, which depends on the momentum fraction $x_a(x_b)$, the factorization scale μ_F and on the renormalization scale μ_R. We take $\mu_F = \mu_R$. The parton level Mandelstam variables $\hat{s}$, $\hat{t}$, and $\hat{u}$ can be expressed in terms of x_a, x_b as

$$\begin{aligned}
\hat{s} &= x_a \, x_b \, s \\
\hat{t} &= M^2 - x_a \, \sqrt{s} \, m_T \, e^{-y} \\
\hat{u} &= M^2 - x_b \, \sqrt{s} \, m_T \, e^{y},
\end{aligned} \quad (2)$$

where $\sqrt{s}$ being the total energy in the centre-of-mass, y is the rapidity and p_T is the transverse momentum of the $Q\bar{Q}$ pair. Writing down $\hat{s} + \hat{t} + \hat{u} - M^2 = 0$ and solving for x_b we obtain

$$x_b = \frac{1}{\sqrt{s}} \frac{x_a \sqrt{s} \, m_T \, e^{-y} - m_H^2}{x_a \sqrt{s} - m_T \, e^{y}}. \quad (3)$$

The double differential cross-section upon p_T and y then takes the following form

$$\frac{d^2\sigma^{ab\to cd}}{dp_T \, dy} = \sum_{a,b} \int_{x_a^{min}}^1 dx_a \, G_{a/A}(x_a, \mu_F^2) \, G_{b/B}(x_b, \mu_F^2) \times 2p_T \frac{x_a \, x_b}{x_a - \frac{m_T}{\sqrt{s}} e^y} \frac{d\sigma}{d\hat{t}}, \quad (4)$$

where the minimum value of x_a is given by

$$x_{a\min} = \frac{1}{\sqrt{s}} \frac{\sqrt{s} \, m_T \, e^y - m_H^2}{\sqrt{s} - m_T \, e^{-y}}. \quad (5)$$

The parton level cross-section $d\sigma/d\hat{t}$ is defined as []

$$\frac{d\sigma}{d\hat{t}} = \frac{d\sigma}{d\hat{t}}(ab \to Q\bar{Q}(^{2S+1}L_J) + X) \, M_L(Q\bar{Q}(^{2S+1}L_J) \to \psi). \quad (6)$$

The short distance contribution $d\sigma/d\hat{t}(ab \to Q\bar{Q}(^{2S+1}L_J) + X)$ correspond to the production of a $Q\bar{Q}$ pair in a particular color and spin configuration can be calculated within

4

the framework of perturbative QCD (pQCD). The long distance matrix elements (LDME) $M_L(Q\overline{Q}(^{2S+1}L_J) \to \psi)$ corresponds to the probability of the $Q\bar{Q}$ state to convert to the quarkonium wavefunction and can be estimated by comparison with experimental measurements. The short distance invariant differential cross-section is given by

$$\frac{d\sigma}{d\hat{t}}(ab \to Q\overline{Q}(^{2S+1}L_J) + X) = \frac{|\mathcal{M}|^2}{16\pi\hat{s}^2}, \tag{7}$$

where $|\mathcal{M}|^2$ is the feynman squared amplitude. We use the expressions for the short distance Color Singlet (CS) cross-sections given in Refs. [35–37] and the Color Octet (CO) cross-sections given in Refs. [38–40]. The CTEQ6M [41] parameterizations are used for parton distribution functions.

The LDMEs scale with a definite power of the relative velocity v of the heavy quarks inside $Q\bar{Q}$ bound states. In the limit $v << 1$, the production of quarkonium is based on the $^3S_1^{[1]}$ and $^3P_J^{[1]}$ ($J = 0,1,2$) CS states and $^1S_0^{[8]}$, $^3S_1^{[8]}$ and $^3P_J^{[8]}$ CO states. The differential cross section for the direct production of J/ψ can be written as the sum of these contributions,

$$d\sigma(J/\psi) = d\sigma(Q\bar{Q}([^3S_1]_1)) M_L(Q\bar{Q}([^3S_1]_1) \to J/\psi) + d\sigma(Q\bar{Q}([^1S_0]_8)) M_L(Q\bar{Q}([^1S_0]_8) \to J/\psi)$$
$$+ d\sigma(Q\bar{Q}([^3S_1]_8)) M_L(Q\bar{Q}([^3S_1]_8) \to J/\psi) + d\sigma(Q\bar{Q}([^3P_0]_8)) M_L(Q\bar{Q}([^3P_0]_8) \to J/\psi)$$
$$+ d\sigma(Q\bar{Q}([^3P_1]_8)) M_L(Q\bar{Q}([^3P_1]_8) \to J/\psi) + d\sigma(Q\bar{Q}([^3P_2]_8)) M_L(Q\bar{Q}([^3P_2]_8) \to J/\psi)$$
$$+ \cdots$$
$$\tag{8}$$

The dots represent contribution of terms at higher powers of v. The contributions from the CO matrix elements in Eq. 8 are suppressed by v^4 compared to the CS matrix elements.

For the case of the p-wave bound states χ_{cJ} (χ_{c0}, χ_{c1}, and χ_{c2}) the color-singlet state $Q\bar{Q}[^3P_J]_1$ and the color-octet state $Q\bar{Q}[^3S_1]_8$ contribute to the same order in v (v^5) because of the angular momentum barrier for $p-$wave states, and hence both need to be included. The χ_c differential cross section thus can be written as

$$d\sigma(\chi_{cJ}) = d\sigma(Q\bar{Q}([^3P_J]_1)) M_L(Q\bar{Q}([^3P_J]_1) \to \chi_{cJ}) + d\sigma(Q\bar{Q}([^3S_1]_8)) M_L(Q\bar{Q}([^3S_1]_8) \to \chi_{cJ})$$
$$+ \cdots$$
$$\tag{9}$$

Similar expressions hold for the $\chi_b(1P)$, $\chi_b(2P)$ and $\chi_b(3P)$ mesons. The prompt J/ψ production at LHC energies consists of direct J/ψ production from initial parton-parton hard

scattering and feed-down contributions to the J/ψ from the decay of heavier charmonium states $\psi(2S)$, χ_{c0}, χ_{c1} and χ_{c2}. The relevant branching fractions are given in Table I. The prompt $\psi(2S)$ has no significant feed-down contributions from higher mass states.

TABLE I. Relevant branching fractions for charmonia [43]

Meson From	to χ_{c0}	to χ_{c1}	to χ_{c2}	to J/ψ
$\psi(2S)$	0.0962	0.092	0.0874	0.595
χ_{c0}				0.0116
χ_{c1}				0.344
χ_{c2}				0.195

The expressions and the values for the color-singlet operators can be found in [38, 39, 42] which are obtained by solving the non-relativistic wavefunctions:

$$M_L(c\bar{c}([^3S_1]_1) \to J/\psi) = 3\,M_L(c\bar{c}([^1S_0]_1) \to J/\psi) = 3N_c\frac{|R_{n=1}(0)|^2}{2\pi} = 1.2 \text{ GeV}^3 \;,$$

$$M_L(c\bar{c}([^3S_1]_1) \to \psi(2S)) = 3\,M_L(c\bar{c}([^1S_0]_1) \to \psi(2S)) = 3N_c\frac{|R_{n=2}(0)|^2}{2\pi} = 0.76 \text{ GeV}^3 \;,$$

$$\frac{1}{5}M_L(c\bar{c}([^3P_2]_1) \to \chi_{c2}(1P)) = \frac{1}{3}\,M_L(c\bar{c}([^3P_1]_1) \to \chi_{c1}(1P)) = M_L(c\bar{c}([^3P_0]_1) \to \chi_{c0}(1P))$$

$$= 3N_c\frac{|R'_{n=1}(0)|^2}{2\pi} = 0.054\,m_{\text{charm}}^2 \text{ GeV}^3.$$

$$(10)$$

Here $R(0)$ is the radial wavefunction and $R'(0)$ is the first derivative of the radial wavefunction at the origin, and n refers to the radial quantum number. The mass of the charm quark is taken as $m_{charm} = 1.6$ GeV. The color-octet operators can not be related to the non-relativistic wavefunctions of $Q\bar{Q}$ since it involves a higher Fock state. We use measured data from LHC [26–28] and TeVatron [29, 30] to constrain these Color Octet Matrix elements. Yields of $\psi(2S)$ have been measured at TeVatron [29] and LHC [26]. Data for χ_{cJ} are available from TeVatron [31]. The following color-singlet and color-octet contributions are relevant for our calculation.

1. Direct contributions

$$M_L(c\bar{c}([^3S_1]_1) \to J/\psi) = 1.2\,\text{GeV}^3$$

$$M_L(c\bar{c}([^3S_1]_8) \to J/\psi)$$

$$M_L(c\bar{c}([^1S_0]_8) \to J/\psi)$$

$$M_L(c\bar{c}([^3P_0]_8) \to J/\psi)$$

(11)

2. Feed-down contribution from $\psi(2S)$

$$M_L(c\bar{c}([^3S_1]_1) \to \psi(2S)) = 0.76\,\text{GeV}^3$$

$$M_L(c\bar{c}([^3S_1]_8) \to \psi(2S))$$

$$M_L(c\bar{c}([^1S_0]_8) \to \psi(2S))$$

$$M_L(c\bar{c}([^3P_0]_8) \to \psi(2S))$$

(12)

3. Feed-down contribution from χ_{cJ}

$$M_L(c\bar{c}([^3P_0]_1) \to \chi_{c0}) = 0.054\,m_c^2\,\text{GeV}^3$$

$$M_L(c\bar{c}([^3S_1]_8) \to \chi_{c0})$$

(13)

Hence for J/ψ we need to determine 10 parameters. Three color singlet matrix elements can be estimated from the wavefunctions of the heavy mesons. The remaining 7 color-octet components are determined as described below. CDF [31] has measured the feed-down contribution from the χ_{cJ} states to J/ψ which is shown in the Figure 1 along with different fitted components. The value of the color octet matrix element obtained from this fitting is

$$M_L(Q\bar{Q}([^3S_1]_8) \to \chi_{c0})/m_{\text{charm}}^2 = (0.00157 \pm 0.00159)\,\text{GeV}^3\,,$$

(14)

The measured yields of prompt $\psi(2S)$ from the following data sets are used to to obtain color octet $\psi(2S)$ matrix elements.

1. CMS results at $\sqrt{S} = 7$ TeV [26, 27]

2. ATLAS results at $\sqrt{S} = 7$ and 8 TeV [28]

3. CDF results at $\sqrt{S} = 1.8$ TeV [29]

4. CDF results at $\sqrt{S} = 1.96$ TeV [30]

5. LHCb results at $\sqrt{S} = 7$ TeV [34]

Figure 2 and Figure 3 show the fitted values of color-singlet and color-octet cross-section components along with the measured $\psi(2S)$ cross-section. We found following values of $\psi(2S)$ color-octet matrix elements

$$M_L(c\bar{c}([^3S_1]_8) \to \psi(2S)) = (0.00190 \pm 0.00002)\,\text{GeV}^3$$
$$M_L(c\bar{c}([^1S_0]_8) \to \psi(2S)) = (0.0264 \pm 0.0003)\,\text{GeV}^3 \qquad (15)$$
$$= M_L(c\bar{c}([^3P_0]_8) \to \psi(2S))/m_{\text{charm}}^2 \ ,$$

with a $\chi^2/dof = 00$. To fit the remaining 3 parameters we use the combined fit for the following datasets of J/ψ (direct+feed-down) yields

1. CMS results at $\sqrt{S} = 7$ TeV [26, 27]

2. ATLAS results at $\sqrt{S} = 7$ and 8 TeV [28]

3. CDF results at $\sqrt{S} = 1.8$ TeV [29]

4. CDF results at $\sqrt{S} = 1.96$ TeV [30]

5. LHCb results at $\sqrt{S} = 7$ TeV [32]

6. LHCb results at $\sqrt{S} = 13$ TeV [33]

Figure 4 and Figure 5 show the fitted values of color-singlet and color-octet cross-section components along with the measured J/ψ cross-section. Making a simultaneous fit of these data-sets we obtain,

$$M_L(c\bar{c}([^3S_1]_8) \to J/\psi) = (0.00317 \pm 0.00007)\,\text{GeV}^3$$
$$M_L(c\bar{c}([^1S_0]_8) \to J/\psi) = (0.0630 \pm 0.0015)\,\text{GeV}^3 \qquad (16)$$
$$= M_L(c\bar{c}([^3P_0]_8) \to J/\psi)/m_{\text{charm}}^2 \ ,$$

with a $\chi^2/dof = 0$. For a more sophisticated fitting of the color-octet matrix elements including NLO effects, see [21, 24].

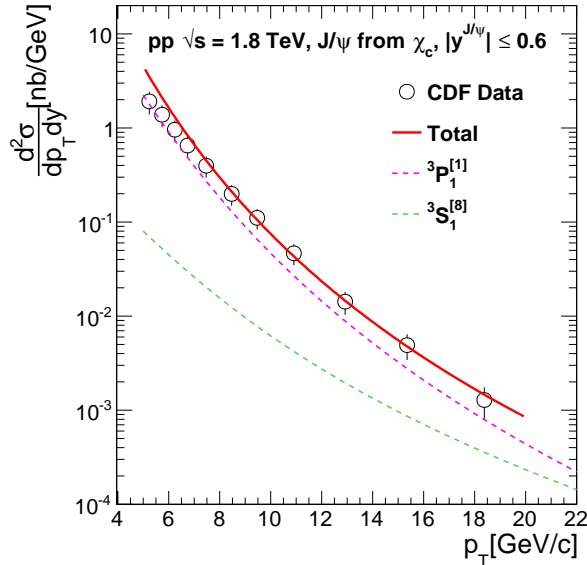FIG. 1. (Color online) Differential production cross-section of J/ψ from χ_{c1} and χ_{c2} decays as a function of J/ψ p_T measured by CDF experiment at $\sqrt{s} = 1.8$ TeV [31]. We use these data sets to constrain color octet LDMEs. Figure also shows our calculations for various components of χ_c cross-section.

III. RESULT AND DISCUSSION

Figure 8 (a) shows the differential production cross-section of prompt J/ψ as a function of transeverse momentum (p_T) compared with the CMS measurements [27]. We have calculated differential production cross-sections for all the relevant resonances. These cross sections are then appropriately scaled with proper branching fractions and total cross section for prompt J/ψ is calculated and shown in Fig. 8 (a). The $\psi(2S)$ has largest contribution at high p_T while at low p_T contribution from χ_{c1} and χ_{c2} exceed the $\psi(2S)$ contribution. After adding all the contributions, the p_T dependence of prompt J/ψ differential production cross-section are described reasonably well by our calculations. The $\psi(2S)$ has no significant feed-down contributions from higher mass states. We call this direct contribution as "prompt $\psi(2S)$" to be consistent with the J/ψ calculations. Figure 8(b) shows the differential production cross-section of prompt $\psi(2S)$ as a function of p_T compared with the CMS measurements [27]. Here also our calculations qualitatively reproduced the mesaured cross section.

Discription for old figures, should put new figures of cross section prediction at 14 TeV and describe the fitting figures.
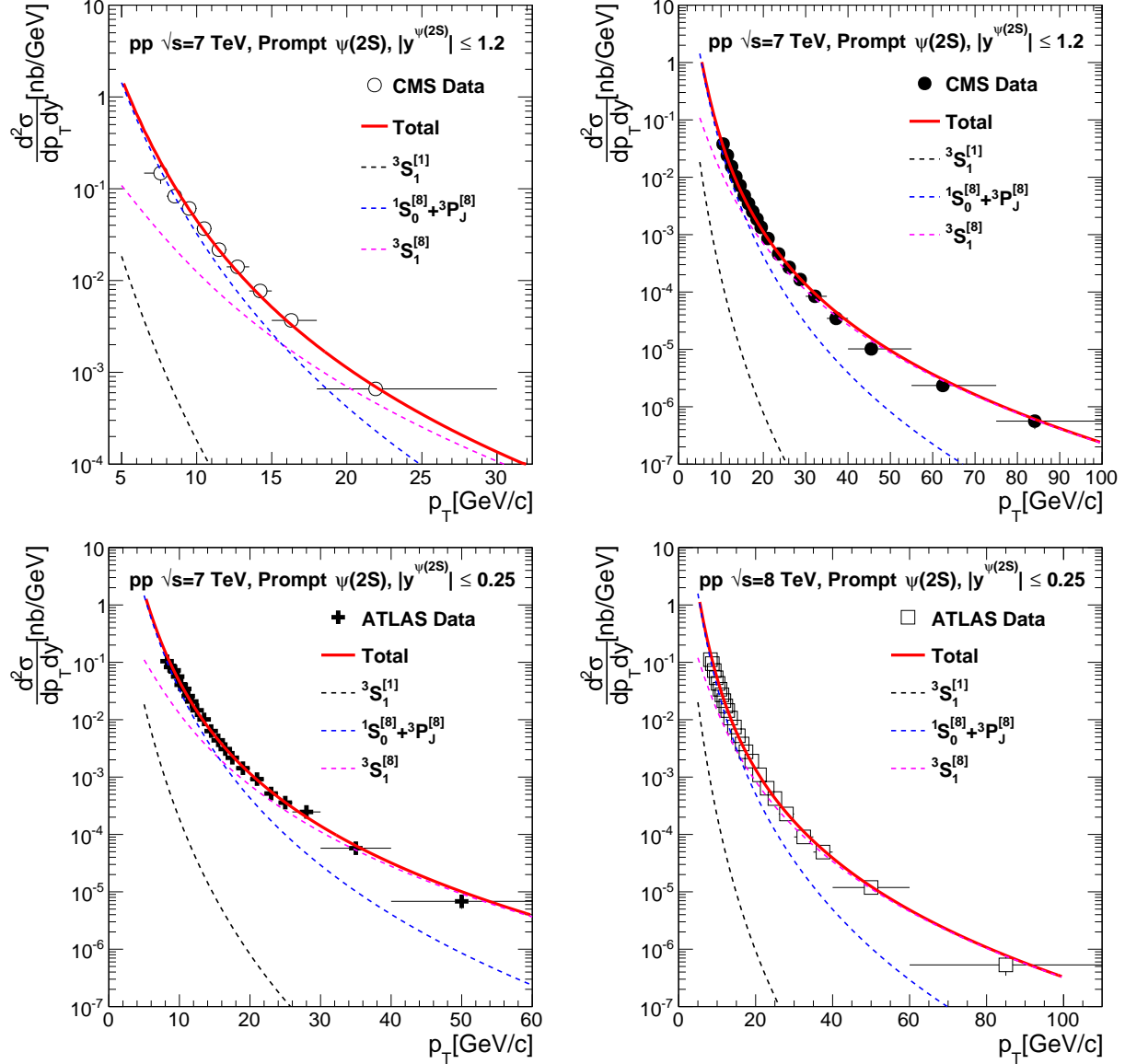
FIG. 2. (Color online) Differential production cross-section of $\psi(2S)$ as a function of p_T collected by LHC experiments at $\sqrt{s} = 7$ and 8 TeV [26–28]. We use these data sets to constrain color octet LDMEs. Figures also shows our calculations for various components of $\psi(2S)$ cross-section.

IV. SUMMARY

We have calculated the differential production cross-section of prompt J/ψ and prompt $\psi(2S)$ as a function of transverse momentum. For the J/ψ meson all the relevent contributions from higher mass states are estimated. The $\psi(2S)$ meson does not have significant contributions from higher mass states. The calculations for prompt J/ψ and prompt $\psi(2S)$
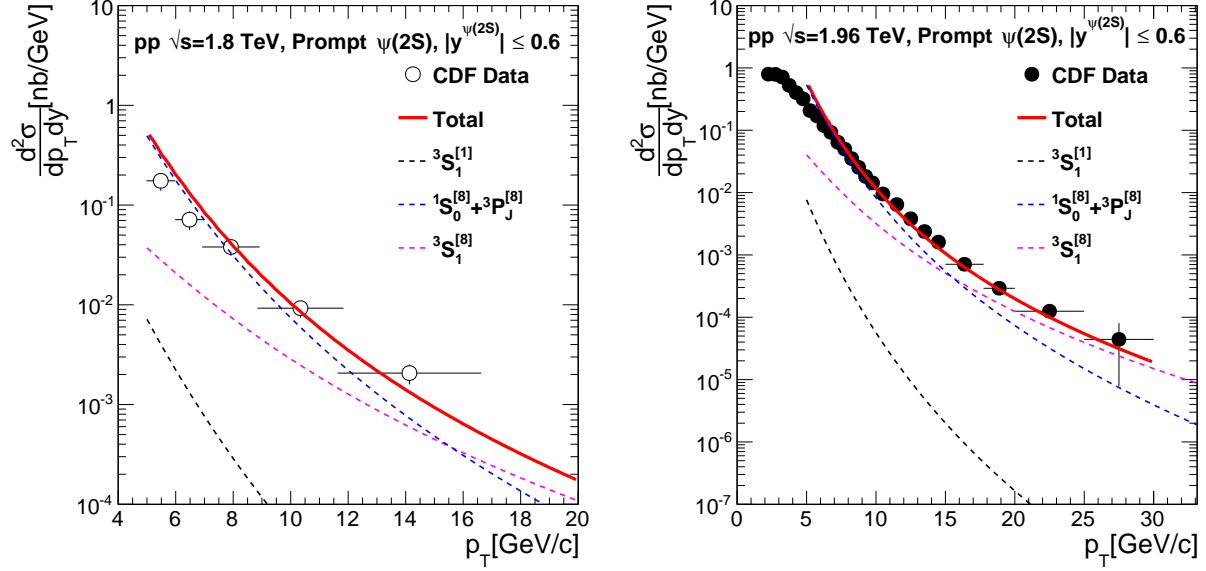
FIG. 3. (Color online) Differential production cross-section of $\psi(2S)$ as a function of p_T collected by CDF experiment at $\sqrt{s} = 1.8$ TeV [29] and $\sqrt{s} = 1.96$ TeV [30]. We use these data sets to constrain color octet LDMEs. Figures also shows our calculations for various components of $\psi(2S)$ cross-section.

are compared with the measured data at LHC. A fairly good agreement between measured data and calculations is observed in low p_T range. The reevaluation of LDME is in progress using latest data from LHC to achieve good description of data in the whole p_T range.
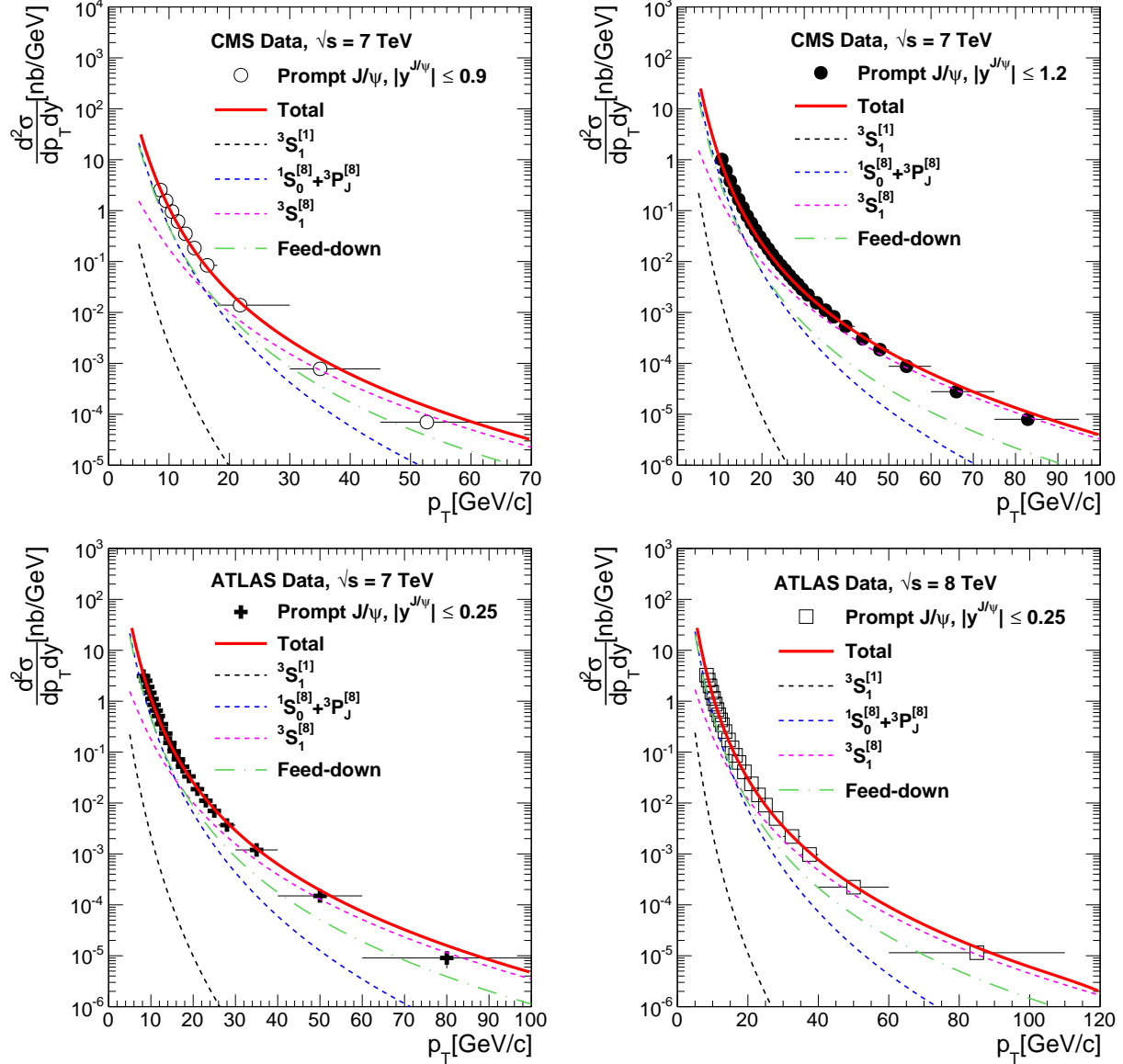
FIG. 4. (Color online) Differential production cross-section of J/ψ as a function of p_T collected by LHC experiments at $\sqrt{s} = 7$ and 8 TeV [26–28]. We use these data sets to constrain color octet LDMEs. Figures also shows our calculations for various components of J/ψ cross-section and feed-down contribution from higher charmonia states.

Appendix A: Short distance pQCD cross sections for quarkonia production

Here we list the lowest order QCD cross sections for the resonance production used in our calculations. We write the formulas in terms of the invariants $\hat{s}$, $\hat{t}$, $\hat{u}$. where $\hat{s}^2 + \hat{t}^2 + \hat{u}^2 = M^2$ and M is the mass of the resonance considered. To order α_s^2 one only has the gluon fusion
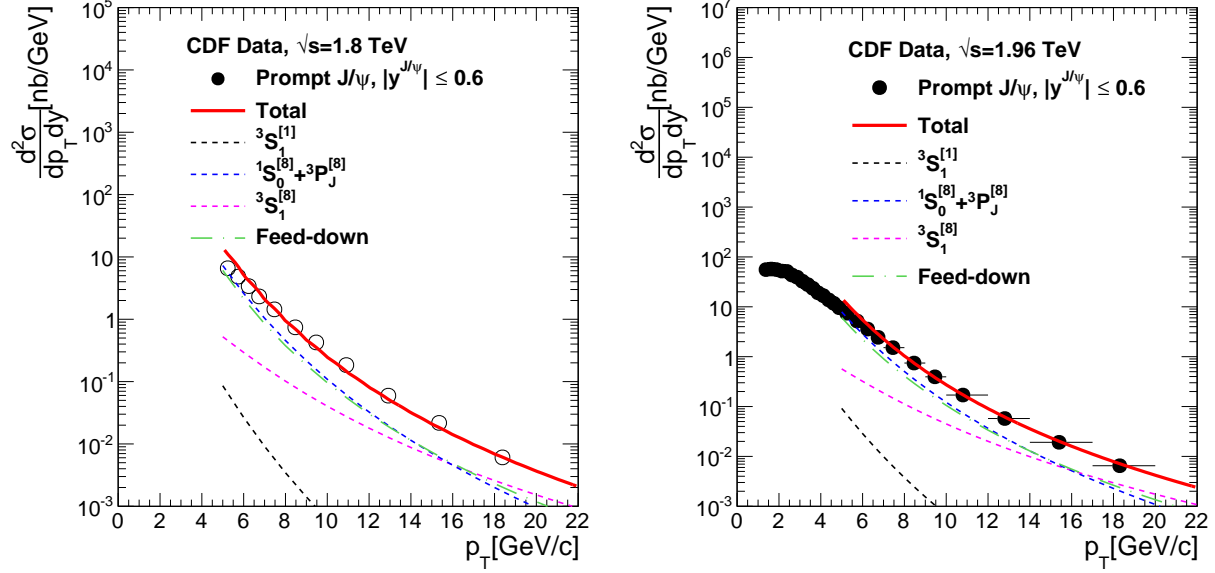
FIG. 5. (Color online) Differential production cross-section of J/ψ as a function of p_T collected by CDF experiment at $\sqrt{s} = 1.8$ TeV [29] and $\sqrt{s} = 1.96$ TeV [30]. We use these data sets to constrain color octet LDMEs. Figures also shows our calculations for various components of J/ψ cross-section and feed-down contribution from higher charmonia states.

FIG. 6. (Color online) Differential production cross-section of J/ψ as a function of p_T collected by LHCb experiment at $\sqrt{s} = 7$ TeV [32] and $\sqrt{s} = 13$ TeV [33]. We use these data sets to constrain color octet LDMEs. Figures also shows our calculations for various components of J/ψ cross-section and feed-down contribution from higher charmonia states.
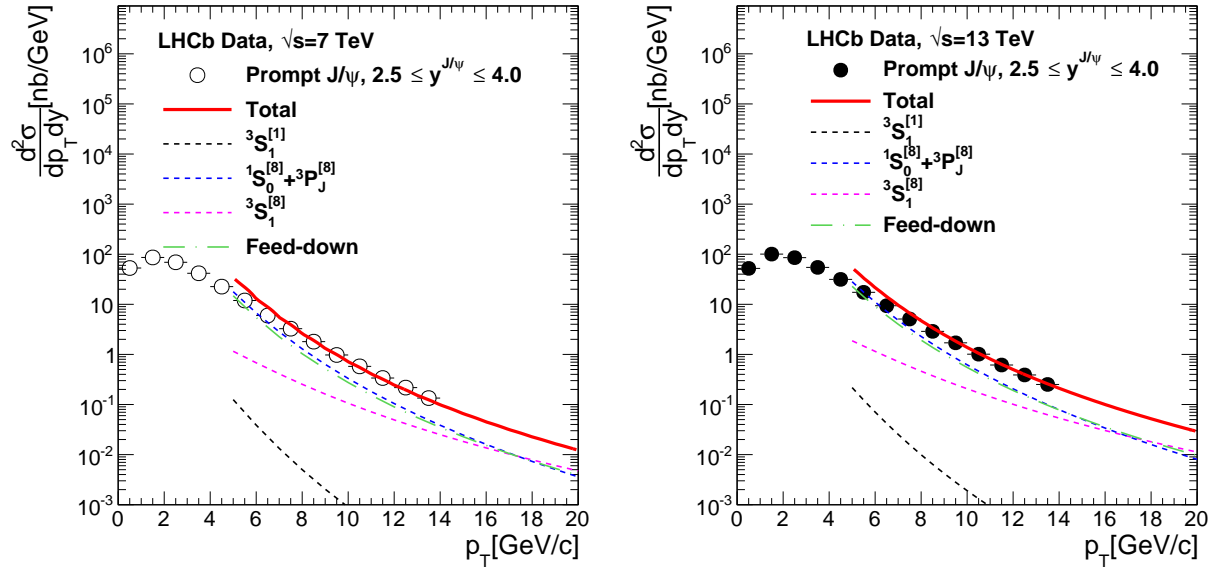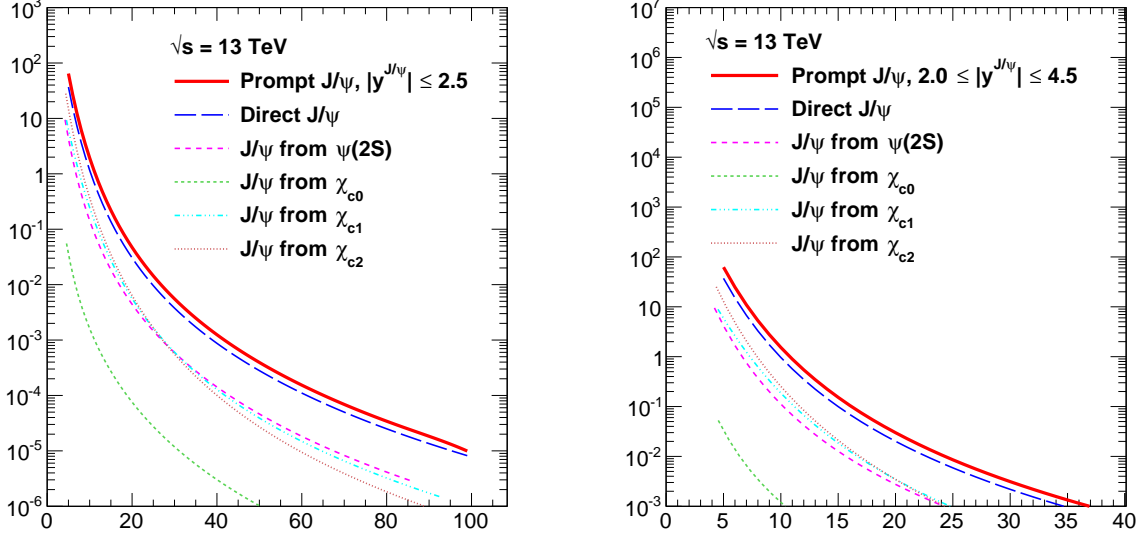
13

FIG. 7. (Color online) Differential production cross-section of J/ψ as a function of p_T predicted by our calculation at $\sqrt{s} = 13$ TeV.
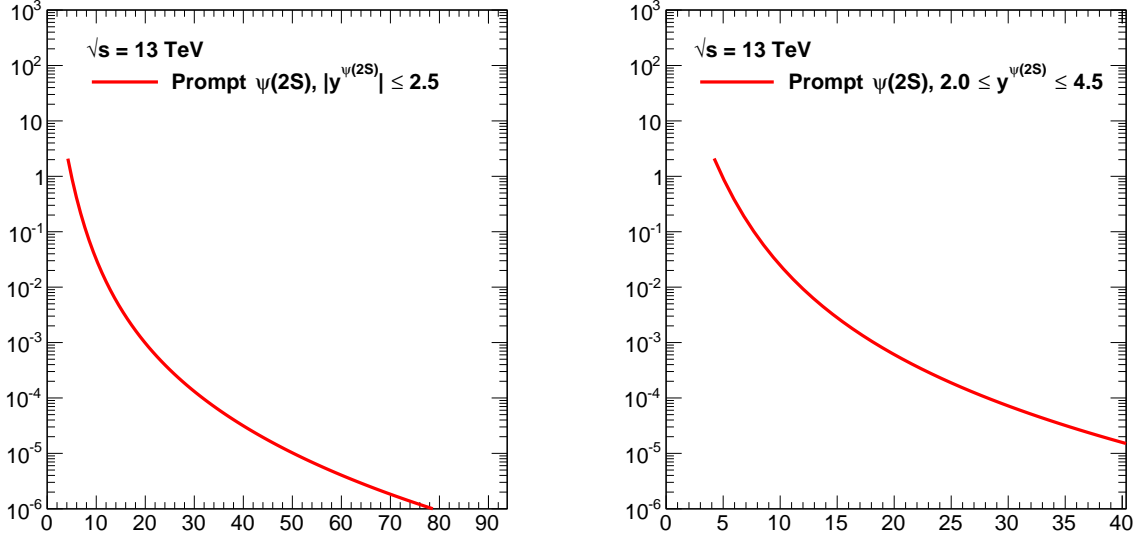
FIG. 8. (Color online) Differential production cross-section of $psi(2S)$ as a function of p_T predicted by our calulation at $\sqrt{s} = 13$ TeV.

processes, g g $\rightarrow^{(2S+1)} L_J$. This process gives resonance with very small p_T, so we do not use these cross-sections in our calculations. To order α_s^3, on the other hand, one has typically two-by-two scattering processes. The relevant cross sections are given below:

14

a.   Color Singlet PQCD cross sections

- g q $\to$ $^{(2S+1)}$L$_J$ q or (q$\to$ q̄)

$$\frac{d\sigma}{d\hat{t}}(^1S_0) = \frac{2\pi\alpha_s{}^3(R_0)^2}{9M\hat{s}^2} \cdot \frac{(\hat{t}-M^2)^2 - 2\hat{s}\hat{u}}{(-\hat{t})(\hat{t}-M^2)^2}$$

$$\frac{d\sigma}{d\hat{t}}(^3P_0) = \frac{8\pi\alpha_s{}^3(R_1')^2}{9M^3\hat{s}^2} \cdot \frac{(\hat{t}-3M^2)^2(\hat{s}^2+\hat{u}^2)}{(-\hat{t})(\hat{t}-M^2)^4}$$

$$\frac{d\sigma}{d\hat{t}}(^3P_1) = \frac{16\pi\alpha_s{}^3(R_1')^2}{3M^3\hat{s}^2} \cdot \frac{-\hat{t}(\hat{s}^2+\hat{u}^2) - 4M^2\hat{s}\hat{u}}{(\hat{t}-M^2)^4} \tag{A1}$$

$$\frac{d\sigma}{d\hat{t}}(^3P_2) = \frac{16\pi\alpha_s{}^3(R_1')^2}{9M^3\hat{s}^2} \cdot$$

$$\frac{(\hat{t}-M^2)^2(\hat{t}^2+6M^4) - 2\hat{s}\hat{u}(\hat{t}^2 - 6M^2(\hat{t}-M^2))}{(-\hat{t})(\hat{t}-M^2)^4}$$

- q q̄ $\to$ $^{(2S+1)}$L$_J$ g

$$\frac{d\sigma}{d\hat{t}}(^{(2S+1)}L_J) = -\frac{8}{3}\frac{\hat{t}^2}{\hat{s}^2}\frac{d\sigma}{d\hat{t}}(gq \to{}^{(2S+1)} L_Jq)|_{\hat{t}\leftrightarrow\hat{u}} \tag{A2}$$

- g g $\to$ $^{(2S+1)}$L$_J$ g

$$\frac{d\sigma}{d\hat{t}}(^3S_1) = \frac{5\pi\alpha_s{}^3(R_0)^2}{9M\hat{s}^2} \cdot \frac{M^2}{(\hat{s}-M^2)^2(\hat{t}-M^2)^2(\hat{u}-M^2)^2}$$

$$\cdot \{[\hat{s}^2(\hat{s}-M^2)^2] + [\hat{s}\to\hat{t}] + [\hat{s}\to\hat{u}]\} \tag{A3}$$

$$\frac{d\sigma}{d\hat{t}}(^1S_0) = \frac{\pi\alpha_s{}^3(R_0)^2}{2M\hat{s}^2} \frac{1}{\hat{s}\hat{t}\hat{u}(\hat{s}-M^2)^2(\hat{t}-M^2)^2(\hat{u}-M^2)^2}$$

$$\cdot \{[\hat{s}^4(\hat{s}-M^2)^2((\hat{s}-M^2)^2 + 2M^4)$$

$$- \frac{4}{3}\hat{s}\hat{t}\hat{u}(\hat{s}^2+\hat{t}^2+\hat{u}^2)(\hat{s}-M^2)(\hat{t}-M^2)(\hat{u}-M^2) \tag{A4}$$

$$+ \frac{16}{3}M^2\hat{s}\hat{t}\hat{u}(\hat{s}^2\hat{t}^2 + \hat{s}^2\hat{u}^2 + \hat{t}^2\hat{u}^2)$$

$$+ \frac{28}{3}M^4\hat{s}^2\hat{t}^2\hat{u}^2] + [\hat{s}\leftrightarrow\hat{t}] + [\hat{s}\leftrightarrow\hat{u}]\}$$

We define two new variables as a combination of $\hat{s}$, $\hat{t}$ and $\hat{u}$ which can be used to define the g g $\to$ $^{(2S+1)}$L$_J$ g cross sections.

$$P = \hat{s}\hat{t} + \hat{t}\hat{u} + \hat{u}\hat{s}$$

$$Q = \hat{s}\hat{t}\hat{u} \tag{A5}$$

15

$$\frac{d\sigma}{d\hat{t}}(^1S_0) = \frac{\pi\alpha_s{}^3(R_0)^2}{M\hat{s}^2}\frac{P^2(M^8 - 2M^4P + P^2 + 2M^2Q)}{Q(Q - M^2P)^2}$$

$$\frac{d\sigma}{d\hat{t}}(^3S_1) = \frac{10\pi\alpha_s{}^3(R_0)^2}{9\hat{s}^2}\frac{M(P^2 - M^2Q)}{(Q - M^2P)^2}$$

(A6)

$$\frac{d\sigma}{d\hat{t}}(^1P_1) = \frac{40\pi\alpha_s{}^3(R_1')^2}{3M\hat{s}^2}\frac{[-M^{10}P + M^6P^2 + Q(5M^8 - 7M^4P + 2P^2) + 4M^2Q^2]}{(Q - M^2P)^3}$$

$$\frac{d\sigma}{d\hat{t}}(^3P_0) = \frac{4\pi\alpha_s{}^3(R_1')^2}{M^3\hat{s}^2}\frac{1}{Q(Q - M^2P)^4}[9M^4P^4(M^8 - 2M^4P + P^2)$$

$$- 6M^2P^3Q(2M^8 - 5M^4P + P^2)$$

$$- P^2Q^2(M^8 + 2M^4P - P^2)$$

$$+ 2M^2PQ^3(M^4 - P) + 6M^4Q^4]$$

(A7)

$$\frac{d\sigma}{d\hat{t}}(^3P_1) = \frac{12\pi\alpha_s{}^3(R_1')^2}{M^3\hat{s}^2}\frac{P^2\{M^2P^2(M^4 - 4P) - 2Q(M^8 - 5M^4P - P^2) - 15M^2Q^2\}}{(Q - M^2P)^4}$$

$$\frac{d\sigma}{d\hat{t}}(^3P_2) = \frac{4\pi\alpha_s{}^3(R_1')^2}{M^3\hat{s}^2}\frac{1}{Q(Q - M^2P)^4}$$

$$\{12M^4P^4(M^8 - 2M^4P + P^2) - 3M^2P^3Q(8M^8 - M^4P + 4P^2)$$

$$- 2P^2Q^2(7M^8 - 43M^4P - P^2) + M^2PQ^3(16M^4 - 61P)$$

$$+ 12M^4Q^4\}$$

(A8)

b. Color Octet PQCD cross sections

We list below short distance squared amplitudes for $2 \rightarrow 2$ scattering processes which mediate color-octet quarkonia production. These expressions are averaged over initial spins and colors of the two incident partons. The helicity levels of outgoing $J = 1$ and $J = 2$ pairs are labeled by the subscript h.

- q q̄ $\rightarrow Q\bar{Q}[^{(2S+1)}L_J^{(8)}]$ g

$$\overline{\sum}|\mathcal{A}(q\bar{q} \rightarrow Q\overline{Q}[^1S_0^{(8)}]g)|^2 = \frac{5(4\pi\alpha_s)^3}{27M}\frac{\hat{t}^2 + \hat{u}^2}{\hat{s}(\hat{s} - M^2)^2}$$

$$\sum_{h=0}\overline{}|\mathcal{A}(q\bar{q} \rightarrow Q\overline{Q}[^3S_1^{(8)}]g)|^2 = \frac{8(4\pi\alpha_s)^3}{81M^3}\frac{M^2\hat{s}}{(\hat{s} - M^2)^4}[4(\hat{t}^2 + \hat{u}^2) - \hat{t}\hat{u}]$$

(A9)

$$\sum_{|h|=1}\overline{}|\mathcal{A}(q\bar{q} \rightarrow Q\overline{Q}[^3S_1^{(8)}]g)|^2 = \frac{2(4\pi\alpha_s)^3}{81M^3}\frac{\hat{s}^2 + M^4}{(\hat{s} - M^2)^4}\frac{\hat{t}^2 + \hat{u}^2}{\hat{t}\hat{u}}[4(\hat{t}^2 + \hat{u}^2) - \hat{t}\hat{u}]$$

16

$$\overline{\sum} |\mathcal{A}(q\bar{q} \to Q\overline{Q}[^3P_0^{(8)}]g)|^2 = \frac{20(4\pi\alpha_s)^3}{81M^3} \frac{(\hat{s} - 3M^2)^2(\hat{t}^2 + \hat{u}^2)}{\hat{s}(\hat{s} - M^2)^4}$$

$$\overline{\sum_{h=0}} |\mathcal{A}(q\bar{q} \to Q\overline{Q}[^3P_1^{(8)}]g)|^2 = \frac{40(4\pi\alpha_s)^3}{81M^3} \frac{\hat{s}(\hat{t}^2 + \hat{u}^2)}{(\hat{s} - M^2)^4} \qquad \text{(A10)}$$

$$\overline{\sum_{|h|=1}} |\mathcal{A}(q\bar{q} \to Q\overline{Q}[^3P_1^{(8)}]g)|^2 = \frac{160(4\pi\alpha_s)^3}{81M^3} \frac{M^2\hat{t}\hat{u}}{(\hat{s} - M^2)^4}$$

$$\overline{\sum_{h=0}} |\mathcal{A}(q\bar{q} \to Q\overline{Q}[^3P_2^{(8)}]g)|^2 = \frac{8(4\pi\alpha_s)^3}{81M^3} \frac{\hat{s}(\hat{t}^2 + \hat{u}^2)}{(\hat{s} - M^2)^4}$$

$$\overline{\sum_{|h|=1}} |\mathcal{A}(q\bar{q} \to Q\overline{Q}[^3P_2^{(8)}]g)|^2 = \frac{32(4\pi\alpha_s)^3}{27M^3} \frac{M^2\hat{t}\hat{u}}{(\hat{s} - M^2)^4} \qquad \text{(A11)}$$

$$\overline{\sum_{|h|=2}} |\mathcal{A}(q\bar{q} \to Q\overline{Q}[^3P_2^{(8)}]g)|^2 = \frac{16(4\pi\alpha_s)^3}{27M^3} \frac{M^4(\hat{t}^2 + \hat{u}^2)}{\hat{s}(\hat{s} - M^2)^4}$$

- g q $\to Q\bar{Q}[^{(2S+1)}\mathrm{L}_\mathrm{J}^{(8)}]$ q

$$\overline{\sum}|\mathcal{A}(gq \to Q\overline{Q}[^1S_0^{(8)}]q)|^2 = -\frac{5(4\pi\alpha_s)^3}{72M}\frac{\hat{s}^2 + \hat{u}^2}{\hat{t}(\hat{t}-M^2)^2}$$

$$\overline{\sum_{h=0}}|\mathcal{A}(gq \to Q\overline{Q}[^3S_1^{(8)}]q)|^2 = -\frac{(4\pi\alpha_s)^3}{54M^3}\frac{M^2\hat{t}\big[4(\hat{s}^2+\hat{u}^2)-\hat{s}\hat{u}\big]}{\big[(\hat{s}-M^2)(\hat{t}-M^2)\big]^2}$$

$$\overline{\sum_{|h|=1}}|\mathcal{A}(gq \to Q\overline{Q}[^3S_1^{(8)}]q)|^2 = -\frac{(4\pi\alpha_s)^3}{108M^3}$$

$$\times \frac{(\hat{s}^2+\hat{u}^2+2M^2\hat{t})(\hat{s}-M^2)^2 - 2M^2\hat{s}\hat{t}\hat{u}}{\hat{s}\hat{u}\big[(\hat{s}-M^2)(\hat{t}-M^2)\big]^2}$$

$$\times \big[4(\hat{s}^2+\hat{u}^2)-\hat{s}\hat{u}\big]$$

$$\overline{\sum}|\mathcal{A}(gq \to Q\overline{Q}[^3P_0^{(8)}]q)|^2 = -\frac{5(4\pi\alpha_s)^3}{54M^3}\frac{(\hat{t}-3M^2)^2(\hat{s}^2+\hat{u}^2)}{\hat{t}(\hat{t}-M^2)^4}$$

$$\overline{\sum_{h=0}}|\mathcal{A}(gq \to Q\overline{Q}[^3P_1^{(8)}]q)|^2 = -\frac{5(4\pi\alpha_s)^3}{27M^3}\frac{\hat{t}\big[\hat{s}^2(\hat{s}-M^2)^2 + \hat{u}^2(\hat{s}+M^2)^2\big]}{(\hat{t}-M^2)^4(\hat{s}-M^2)^2}$$

$$\overline{\sum_{|h|=1}}|\mathcal{A}(gq \to Q\overline{Q}[^3P_1^{(8)}]q)|^2 = -\frac{20(4\pi\alpha_s)^3}{27M^3}\frac{M^2\hat{s}\hat{u}(\hat{t}^2+\hat{t}\hat{u}+\hat{u}^2)}{(\hat{t}-M^2)^4(\hat{s}-M^2)^2}$$

$$\overline{\sum_{h=0}}|\mathcal{A}(gq \to Q\overline{Q}[^3P_2^{(8)}]q)|^2 = -\frac{(4\pi\alpha_s)^3}{27M^3}\frac{\hat{t}}{(\hat{t}-M^2)^4}$$

$$\times \Big[\hat{s}^2 + \hat{u}^2 + 12M^2\hat{s}\hat{u}^2\frac{\hat{s}^2 + M^2\hat{s} + M^4}{(\hat{s}-M^2)^4}\Big]$$

$$\overline{\sum_{|h|=1}}|\mathcal{A}(gq \to Q\overline{Q}[^3P_2^{(8)}]q)|^2 = -\frac{4(4\pi\alpha_s)^3}{9M^3}\frac{M^2\hat{s}\hat{u}}{(\hat{t}-M^2)^4}$$

$$\times \frac{(\hat{s}-M^2)^2(\hat{s}^2+M^4) - (\hat{s}+M^2)^2\hat{t}\hat{u}}{(\hat{s}-M^2)^4}$$

$$\overline{\sum_{|h|=2}}|\mathcal{A}(gq \to Q\overline{Q}[^3P_2^{(8)}]q)|^2 = -\frac{2(4\pi\alpha_s)^3}{9M^3}\frac{M^4}{\hat{t}(\hat{t}-M^2)^4}$$

$$\times \Big[\hat{s}^2 + \hat{u}^2 + 2\hat{s}^2\hat{t}\hat{u}\frac{(\hat{s}-M^2)(2\hat{t}+\hat{u}) - \hat{u}^2}{(\hat{s}-M^2)^4}\Big]$$

(A12)

- g g $\to Q\bar{Q}[^{(2S+1)}\mathrm{L}_\mathrm{J}^{(8)}]$ g (The $gg \to Q\overline{Q}[^3P_J^{(8)}]$ g squared amplitudes are expressed in

18

terms of the variables $\hat{s}$ and $\hat{z} \equiv \sqrt{\hat{t}\hat{u}}$.)

$$\sum |\mathcal{A}(gg \to Q\overline{Q}[^1S_0^{(8)}]g)|^2 = \frac{5(4\pi\alpha_s)^3}{16M}\left[\hat{s}^2(\hat{s}-M^2)^2 + \hat{s}\hat{t}\hat{u}(M^2 - 2\hat{s}) + (\hat{t}\hat{u})^2\right]$$
$$\times \frac{(\hat{s}^2 - M^2\hat{s} + M^4)^2 - \hat{t}\hat{u}(2\hat{t}^2 + 3\hat{t}\hat{u} + 2\hat{u}^2)}{\hat{s}\hat{t}\hat{u}\left[(\hat{s}-M^2)(\hat{t}-M^2)(\hat{u}-M^2)\right]^2}$$

$$\sum_{h=0} |\mathcal{A}(gg \to Q\overline{Q}[^3S_1^{(8)}]g)|^2 = -\frac{(4\pi\alpha_s)^3}{144M^3}\frac{2M^2\hat{s}}{(\hat{s}-M^2)^2}(\hat{t}^2 + \hat{u}^2)\hat{t}\hat{u}$$
$$\times \frac{27(\hat{s}\hat{t} + \hat{t}\hat{u} + \hat{u}\hat{s}) - 19M^4}{\left[(\hat{s}-M^2)(\hat{t}-M^2)(\hat{u}-M^2)\right]^2}$$

$$\sum_{|h|=1} |\mathcal{A}(gg \to Q\overline{Q}[^3S_1^{(8)}]g)|^2 = -\frac{(4\pi\alpha_s)^3}{144M^3}\frac{\hat{s}^2}{(\hat{s}-M^2)^2}$$
$$\times \left[(\hat{s}-M^2)^4 + \hat{t}^4 + \hat{u}^4 + 2M^4\left(\frac{\hat{t}\hat{u}}{\hat{s}}\right)^2\right]$$
$$\times \frac{27(\hat{s}\hat{t} + \hat{t}\hat{u} + \hat{u}\hat{s}) - 19M^4}{\left[(\hat{s}-M^2)(\hat{t}-M^2)(\hat{u}-M^2)\right]^2}$$

$$\sum |\mathcal{A}(gg \to Q\overline{Q}[^3P_0^{(8)}]g)|^2 = \frac{5(4\pi\alpha_s)^3}{12M^3}\frac{1}{\left[\hat{s}\hat{z}^2(\hat{s}-M^2)^4(\hat{s}M^2 + \hat{z}^2)^4\right]}$$
$$\times \left\{\hat{s}^2\hat{z}^4(\hat{s}^2 - \hat{z}^2)^4 + M^2\hat{s}\hat{z}^2(\hat{s}^2 - \hat{z}^2)^2(3\hat{s}^2 - 2\hat{z}^2)(2\hat{s}^4 - 6\hat{s}^2\hat{z}^2 + 3\hat{z}^4)\right.$$
$$+ M^4\left[9\hat{s}^{12} - 84\hat{s}^{10}\hat{z}^2 + 265\hat{s}^8\hat{z}^4 - 382\hat{s}^6\hat{z}^6 + 276\hat{s}^4\hat{z}^8 - 88\hat{s}^2\hat{z}^{10} + 9\hat{z}^{12}\right]$$
$$- M^6\hat{s}\left[54\hat{s}^{10} - 357\hat{s}^8\hat{z}^2 + 844\hat{s}^6\hat{z}^4 - 898\hat{s}^4\hat{z}^6 + 439\hat{s}^2\hat{z}^8 - 81\hat{z}^{10}\right]$$
$$+ M^8\left[153\hat{s}^{10} - 798\hat{s}^8\hat{z}^2 + 1415\hat{s}^6\hat{z}^4 - 1041\hat{s}^4\hat{z}^6 + 301\hat{s}^2\hat{z}^8 - 18\hat{z}^{10}\right]$$
$$- M^{10}\hat{s}\left[270\hat{s}^8 - 1089\hat{s}^6\hat{z}^2 + 1365\hat{s}^4\hat{z}^4 - 616\hat{s}^2\hat{z}^6 + 87\hat{z}^8\right]$$
$$+ M^{12}\left[324\hat{s}^8 - 951\hat{s}^6\hat{z}^2 + 769\hat{s}^4\hat{z}^4 - 189\hat{s}^2\hat{z}^6 + 9\hat{z}^8\right]$$
$$- 9M^{14}\hat{s}\left[(6\hat{s}^2 - \hat{z}^2)(5\hat{s}^4 - 9\hat{s}^2\hat{z}^2 + 3\hat{z}^4)\right]$$
$$+ 3M^{16}\hat{s}^2\left[51\hat{s}^4 - 59\hat{s}^2\hat{z}^2 + 12\hat{z}^4\right]$$
$$- 27M^{18}\hat{s}^3\left[2\hat{s}^2 - \hat{z}^2\right]$$
$$\left.+ 9M^{20}\hat{s}^4\right\}$$

$$(A13)$$

$$\sum_{h=0}^{-} |\mathcal{A}(gg \to Q\overline{Q}[^3P_1^{(8)}]g)|^2 = \frac{5(4\pi\alpha_s)^3}{6M^3} \frac{1}{\left[(\hat{s} - M^2)^4(\hat{s}M^2 + \hat{z}^2)^4\right]}$$

$$\times \hat{s}\hat{z}^2\left[(\hat{s}^2 - \hat{z}^2)^2 - 2M^2\hat{s}\hat{z}^2 - M^4(\hat{s}^2 + 2\hat{z}^2) + M^8\right]$$

$$\times \left[(\hat{s}^2 - \hat{z}^2)^2 - M^2\hat{s}(2\hat{s}^2 - \hat{z}^2) + M^4\hat{s}^2\right]$$

$$\sum_{|h|=1}^{-} |\mathcal{A}(gg \to Q\overline{Q}[^3P_1^{(8)}]g)|^2 = \frac{5(4\pi\alpha_s)^3}{6M^3} \frac{1}{\left[(\hat{s} - M^2)^4(\hat{s}M^2 + \hat{z}^2)^4\right]}$$

$$\times M^2\Big\{2(\hat{s}^2 - \hat{z}^2)^2(\hat{s}^6 - 4\hat{s}^4\hat{z}^2 + \hat{s}^2\hat{z}^4 - \hat{z}^6)$$

$$- M^2\hat{s}(2\hat{s}^2 - \hat{z}^2)(5\hat{s}^6 - 17\hat{s}^4\hat{z}^2 + 9\hat{s}^2\hat{z}^4 - \hat{z}^6)$$

$$+ M^4(21\hat{s}^8 - 49\hat{s}^6\hat{z}^2 + 21\hat{s}^4\hat{z}^4 - 4\hat{s}^2\hat{z}^6 + \hat{z}^8)$$

$$- M^6\hat{s}(24\hat{s}^6 - 30\hat{s}^4\hat{z}^2 + 6\hat{s}^2\hat{z}^4 - \hat{z}^6)$$

$$+ M^8\hat{s}^2(16\hat{s}^4 - 9\hat{s}^2\hat{z}^2 + 2\hat{z}^4)$$

$$- M^{10}\hat{s}^3(6\hat{s}^2 - \hat{z}^2) \tag{A14}$$

$$+ M^{12}\hat{s}^4\Big\}$$

$$\sum_{h=0}^{-} |\mathcal{A}(gg \to Q\overline{Q}[^3P_2^{(8)}]g)|^2 = \frac{(4\pi\alpha_s)^3}{6M^3} \frac{\hat{s}\hat{z}^2}{\left[(\hat{s} - M^2)^6(\hat{s}M^2 + \hat{z}^2)^4\right]}$$

$$\Big\{\hat{s}^2(\hat{s}^2 - \hat{z}^2)^4 - M^2\hat{s}\hat{z}^2(\hat{s}^2 - \hat{z}^2)^2(11\hat{s}^2 + 2\hat{z}^2)$$

$$+ M^4\left[\hat{s}^8 - 12\hat{s}^6\hat{z}^2 + 41\hat{s}^4\hat{z}^4 - 20\hat{s}^2\hat{z}^6 + \hat{z}^8\right]$$

$$- M^6\hat{s}\left[4\hat{s}^6 - 26\hat{s}^4\hat{z}^2 - \hat{s}^2\hat{z}^4 - 5\hat{z}^6\right]$$

$$+ M^8\left[29\hat{s}^6 - 114\hat{s}^4\hat{z}^2 + 108\hat{s}^2\hat{z}^4 - 10\hat{z}^6\right]$$

$$- M^{10}\hat{s}\left[65\hat{s}^4 - 104\hat{s}^2\hat{z}^2 - 33\hat{z}^4\right]$$

$$+ M^{12}\left[54\hat{s}^4 - 20\hat{s}^2\hat{z}^2 + 7\hat{z}^4\right]$$

$$- M^{14}\hat{s}\left[23\hat{s}^2 + 5\hat{z}^2\right]$$

$$+ 7M^{16}\hat{s}^2\Big\}$$

$$\overline{\sum_{|h|=1}} |\mathcal{A}(gg \to Q\overline{Q}[^3P_2^{(8)}]g)|^2 = \frac{(4\pi\alpha_s)^3}{2M^3} \frac{M^2}{\left[(\hat{s} - M^2)^6(\hat{s}M^2 + \hat{z}^2)^4\right]}$$

$$\times \left\{ 2\hat{s}^2(\hat{s}^2 - \hat{z}^2)^2(\hat{s}^6 - 4\hat{s}^4\hat{z}^2 + \hat{s}^2\hat{z}^4 - \hat{z}^6) \right.$$

$$- M^2\hat{s}\left[10\hat{s}^{10} - 37\hat{s}^8\hat{z}^2 + 19\hat{s}^6\hat{z}^4 + 11\hat{s}^4\hat{z}^6 - \hat{s}^2\hat{z}^8 - 4\hat{z}^{10}\right]$$

$$+ M^4\left[25\hat{s}^{10} - 61\hat{s}^8\hat{z}^2 + 27\hat{s}^6\hat{z}^4 - 34\hat{s}^4\hat{z}^6 + 23\hat{s}^2\hat{z}^8 - 2\hat{z}^{10}\right]$$

$$- M^6\hat{s}\left[42\hat{s}^8 - 77\hat{s}^6\hat{z}^2 + 41\hat{s}^4\hat{z}^4 - 22\hat{s}^2\hat{z}^6 + 17\hat{z}^8\right]$$

$$+ M^8\left[53\hat{s}^8 - 88\hat{s}^6\hat{z}^2 + 69\hat{s}^4\hat{z}^4 - 68\hat{s}^2\hat{z}^6 + 3\hat{z}^8\right]$$

$$- M^{10}\hat{s}\left[54\hat{s}^6 - 85\hat{s}^4\hat{z}^2 + 60\hat{s}^2\hat{z}^4 - 9\hat{z}^6\right]$$

$$+ M^{12}\hat{s}^2\left[43\hat{s}^4 - 47\hat{s}^2\hat{z}^2 + 20\hat{z}^4\right]$$

$$- M^{14}\hat{s}^3\left[22\hat{s}^2 - 9\hat{z}^2\right]$$

$$\left. + 5M^{16}\hat{s}^4 \right\}$$

$$\overline{\sum_{|h|=2}} |\mathcal{A}(gg \to Q\overline{Q}[^3P_2^{(8)}]g)|^2 = \frac{(4\pi\alpha_s)^3}{2M^3} \frac{M^4}{\left[\hat{s}\hat{z}^2(\hat{s} - M^2)^6(\hat{s}M^2 + \hat{z}^2)^4\right]}$$

$$\times \left\{ 2\hat{s}^2\left[\hat{s}^{12} - 8\hat{s}^{10}\hat{z}^2 + 22\hat{s}^8\hat{z}^4 - 24\hat{s}^6\hat{z}^6 + 10\hat{s}^4\hat{z}^8 - 3\hat{s}^2\hat{z}^{10} + \hat{z}^{12}\right] \right.$$

$$- M^2\hat{s}\left[16\hat{s}^{12} - 102\hat{s}^{10}\hat{z}^2 + 210\hat{s}^8\hat{z}^4 - 153\hat{s}^6\hat{z}^6 + 36\hat{s}^4\hat{z}^8 - 6\hat{s}^2\hat{z}^{10} + 4\hat{z}^{12}\right]$$

$$+ M^4\left[60\hat{s}^{12} - 306\hat{s}^{10}\hat{z}^2 + 482\hat{s}^8\hat{z}^4 - 271\hat{s}^6\hat{z}^6 + 77\hat{s}^4\hat{z}^8 - 18\hat{s}^2\hat{z}^{10} + 2\hat{z}^{12}\right]$$

$$- M^6\hat{s}\left[140\hat{s}^{10} - 573\hat{s}^8\hat{z}^2 + 710\hat{s}^6\hat{z}^4 - 344\hat{s}^4\hat{z}^6 + 91\hat{s}^2\hat{z}^8 - 18\hat{z}^{10}\right]$$

$$+ M^8\left[226\hat{s}^{10} - 741\hat{s}^8\hat{z}^2 + 737\hat{s}^6\hat{z}^4 - 310\hat{s}^4\hat{z}^6 + 77\hat{s}^2\hat{z}^8 - 4\hat{z}^{10}\right]$$

$$- M^{10}\hat{s}\left[264\hat{s}^8 - 686\hat{s}^6\hat{z}^2 + 541\hat{s}^4\hat{z}^4 - 177\hat{s}^2\hat{z}^6 + 25\hat{z}^8\right]$$

$$+ M^{12}\left[226\hat{s}^8 - 452\hat{s}^6\hat{z}^2 + 261\hat{s}^4\hat{z}^4 - 55\hat{s}^2\hat{z}^6 + 2\hat{z}^8\right]$$

$$- M^{14}\hat{s}\left[140\hat{s}^6 - 201\hat{s}^4\hat{z}^2 + 71\hat{s}^2\hat{z}^4 - 6\hat{z}^6\right]$$

$$+ M^{16}\hat{s}^2\left[60\hat{s}^4 - 53\hat{s}^2\hat{z}^2 + 8\hat{z}^4\right]$$

$$- 2M^{18}\hat{s}^3\left[8\hat{s}^2 - 3\hat{z}^2\right]$$

$$\left. + 2M^{20}\hat{s}^4 \right\}$$

$$(A15)$$

[1] J. E. Augustin *et al.* [SLAC-SP-017 Collaboration], "Discovery of a Narrow Resonance in e+ e- Annihilation," Phys. Rev. Lett. **33**, 1406 (1974) [Adv. Exp. Phys. **5**, 141 (1976)].

[2] J. J. Aubert *et al.* [E598 Collaboration], "Experimental Observation of a Heavy Particle J," Phys. Rev. Lett. **33**, 1404 (1974). doi:10.1103/PhysRevLett.33.1404

[3] P. Nason, S. Dawson and R. K. Ellis, "The Total Cross-Section For The Production Of Heavy Quarks In Hadronic Collisions," Nucl. Phys. B **303** (1988) 607;

[4] P. Nason, S. Dawson and R. K. Ellis, "The One Particle Inclusive Differential Cross-Section For Heavy Quark Production In Hadronic Collisions," Nucl. Phys. B **327** (1989) 49 [Erratum-ibid. B **335** (1990) 260].

[5] G. T. Bodwin, E. Braaten, and G. P. Lepage, "Rigorous QCD analysis of inclusive annihilation and production of heavy quarkonium," Phys. Rev. D **51** 1125 (1995), [Erratum-ibid. D **55** 5853 (1997)], arXiv:hep-ph/9407339.

[6] N. Brambilla *et al.*, Heavy quarkonium physics, CERN-2005-005, (CERN, Geneva, 2005), arXiv:hep-ph/0412158.

[7] M. B. Einhorn and S. D. Ellis, "Hadronic Production Of The New Resonances: Probing Gluon Distributions," Phys. Rev. D **12** 2007 (1975).

[8] S. D. Ellis, M. B. Einhorn, and C. Quigg, "Comment On Hadronic Production Of Psions," Phys. Rev. Lett. **36** 1263 (1976)

[9] C. E. Carlson and R. Suaya, "Hadronic Production Of Psi/J Mesons," Phys. Rev. D **14** 3115 (1976).

[10] E. L. Berger and D. L. Jones, "Inelastic Photoproduction of J/psi and Upsilon by Gluons," Phys. Rev. D **23**, 1521 (1981).

[11] G. A. Schuler, "Quarkonium production and decays," [arXiv:hep-ph/9403387].

[12] P. Artoisenet, J. P. Lansberg, and F. Maltoni, "Hadroproduction of J/ψ and υ in association with a heavy-quark pair," Phys. Lett. B **653** 60 (2007), [arXiv:hep-ph/0703129]

[13] J. M. Campbell, F. Maltoni, and F. Tramontano, "QCD corrections to J/psi and Upsilon production at hadron colliders," Phys. Rev. Lett. **98** 252002 (2007), [arXiv:hep-ph/0703113]

[14] P. Artoisenet, J. M. Campbell, J. P. Lansberg, F. Maltoni, and F. Tramontano, "Υ Production at Fermilab Tevatron and LHC Energies," Phys. Rev. Lett. **101** 152001 (2008),

[arXiv:0806.3282 [hep-ph]].

[15] H. Fritzsch, "Producing Heavy Quark Flavors in Hadronic Collisions: A Test of Quantum Chromodynamics," Phys. Lett. B **67**, 217 (1977).

[16] J. F. Amundson, O. J. P. Eboli, E. M. Gregores and F. Halzen, "Colorless states in perturbative QCD: Charmonium and rapidity gaps," Phys. Lett. B **372**, 127 (1996), [hep-ph/9512248].

[17] J. F. Amundson, O. J. P. Eboli, E. M. Gregores and F. Halzen, "Quantitative tests of color evaporation: Charmonium production," Phys. Lett. B **390**, 323 (1997), [hep-ph/9605295].

[18] B. Gong and J. X. Wang, "Next-to-leading-order QCD corrections to J/ψ polarization at Tevatron and Large-Hadron-Collider energies," Phys. Rev. Lett. **100**, 232001 (2008), [arXiv:0802.3727 [hep-ph]].

[19] B. Gong, X. Q. Li and J. X. Wang, "QCD corrections to J/ψ production via color octet states at Tevatron and LHC," Phys. Lett. B **673**, 197 (2009), [Phys. Lett. **693**, 612 (2010)], [arXiv:0805.4751 [hep-ph]].

[20] Y. Q. Ma, K. Wang and K. T. Chao, "QCD radiative corrections to χ_{cJ} production at hadron colliders," Phys. Rev. D **83**, 111503 (2011), [arXiv:1002.3987 [hep-ph]].

[21] M. Butenschoen and B. A. Kniehl, "J/psi polarization at Tevatron and LHC: Nonrelativistic-QCD factorization at the crossroads," Phys. Rev. Lett. **108**, 172002 (2012), [arXiv:1201.1872 [hep-ph]].

[22] K. T. Chao, Y. Q. Ma, H. S. Shao, K. Wang and Y. J. Zhang, "J/ψ Polarization at Hadron Colliders in Nonrelativistic QCD," Phys. Rev. Lett. **108**, 242004 (2012), [arXiv:1201.2675 [hep-ph]].

[23] B. Gong, L. P. Wan, J. X. Wang and H. F. Zhang, "Polarization for Prompt J/ψ and ψ(2S) Production at the Tevatron and LHC," Phys. Rev. Lett. **110**, no. 4, 042002 (2013), [arXiv:1205.6682 [hep-ph]].

[24] M. Butenschoen and B. A. Kniehl, "Reconciling J/ψ production at HERA, RHIC, Tevatron, and LHC with NRQCD factorization at next-to-leading order," Phys. Rev. Lett. **106**, 022003 (2011),[arXiv:1009.5662 [hep-ph]].

[25] Y. Q. Ma, K. Wang and K. T. Chao, "A complete NLO calculation of the J/ψ and ψ' production at hadron colliders," Phys. Rev. D **84**, 114001 (2011), [arXiv:1012.1030 [hep-ph]].

[26] S. Chatrchyan *et al.* [CMS Collaboration], "J/ψ and ψ_{2S} production in *pp* collisions at $\sqrt{s} = 7$ TeV," JHEP **1202**, 011 (2012), [arXiv:1111.1557 [hep-ex]].

[27] V. Khachatryan *et al.* [CMS Collaboration], "Measurement of J/ψ and ψ(2S) Prompt Double-Differential Cross Sections in pp Collisions at $\sqrt{s}$=7TeV," Phys. Rev. Lett. **114**, no. 19, 191802 (2015), [arXiv:1502.04155 [hep-ex]].

[28] G. Aad *et al.* [ATLAS Collaboration], "Measurement of the differential cross-sections of prompt and non-prompt production of J/ψ and ψ(2S) in pp collisions at $\sqrt{s}$ = 7 and 8 TeV with the ATLAS detector," arXiv:1512.03657 [hep-ex].

[29] F. Abe *et al.* [CDF Collaboration], "J/ψ and $\psi(2S)$ production in $p\bar{p}$ collisions at $\sqrt{s}$ = 1.8 TeV," Phys. Rev. Lett. **79**, 572 (1997).

[30] D. Acosta *et al.* [CDF Collaboration], "Measurement of the J/ψ meson and $b-$hadron production cross sections in $p\bar{p}$ collisions at $\sqrt{s}$ = 1960 GeV," Phys. Rev. D **71**, 032001 (2005).

[31] F. Abe *et al.* [CDF Collaboration], "Production of J/ψ mesons from χ_c meson decays in $p\bar{p}$ collisions at $\sqrt{s}$ = 1.8 TeV," Phys. Rev. Lett. **79**, 578 (1997).

[32] R. Aaij *et al.* [LHCb Collaboration], "Measurement of J/ψ production in pp collisions at $\sqrt{s}$ = 7 TeV," Eur. Phys. J. C **71**, 1645 (2011), [arXiv:1103.0423 [hep-ex]].

[33] R. Aaij *et al.* [LHCb Collaboration], "Measurement of forward J/ψ production cross-sections in pp collisions at $\sqrt{s}$ = 13 TeV," JHEP **1510**, 172 (2015), [arXiv:1509.00771 [hep-ex]].

[34] R. Aaij *et al.* [LHCb Collaboration], "Measurement of ψ(2S) meson production in pp collisions at $\sqrt{s}$=7 TeV," Eur. Phys. J. C **72**, 2100 (2012), [arXiv:1204.1258 [hep-ex]].

[35] R. Baier and R. Ruckl, "Hadronic Collisions: A Quarkonium Factory," Z. Phys. C **19**, 251 (1983).

[36] B. Humpert, "Narrow Heavy Resonance Production By Gluons," Phys. Lett. B **184**, 105 (1987).

[37] R. Gastmans, W. Troost and T. T. Wu, "Production of Heavy Quarkonia From Gluons," Nucl. Phys. B **291**, 731 (1987).

[38] P. L. Cho and A. K. Leibovich, "Color octet quarkonia production," Phys. Rev. D **53**, 150 (1996), [hep-ph/9505329].

[39] P. L. Cho and A. K. Leibovich, "Color octet quarkonia production. 2.," Phys. Rev. D **53**, 6203 (1996), [hep-ph/9511315].

[40] E. Braaten, S. Fleming and A. K. Leibovich, "NRQCD analysis of bottomonium production at the Tevatron," Phys. Rev. D **63**, 094006 (2001), [hep-ph/0008091].

[41] H. L. Lai, M. Guzzi, J. Huston, Z. Li, P. M. Nadolsky, J. Pumplin and C.-P. Yuan, "New parton distributions for collider physics," Phys. Rev. D **82**, 074024 (2010), [arXiv:1007.2241 [hep-ph]].

[42] E. J. Eichten and C. Quigg, "Mesons with beauty and charm: Spectroscopy," Phys. Rev. D **49**, 5845 (1994) [hep-ph/9402210].

[43] K. Nakamura *et al.* [Particle Data Group Collaboration], "Review of particle physics," J. Phys. G **37**, 075021 (2010).